Defect Production in Compressed Filament Bundles

Valentin M. Slepukhin[1] and Alex J. Levine[1,2]

[1]*Department of Physics and Astronomy, University of California, Los Angeles, California 90095-1596, USA*
[2]*Department of Chemistry and Biochemistry, University of California, Los Angeles, California 90095-1596, USA*

We discuss the response of biopolymer filament bundles bound by transient cross-linkers to compressive loading. These systems admit a mechanical instability at stresses typically below that of traditional Euler buckling. In this instability, there is thermally activated pair production of topological defects that generate localized regions of bending—kinks. These kinks shorten the bundle's effective length, thereby reducing the elastic energy of the mechanically loaded structure. This effect is the thermal analog of the Schwinger effect, in which a sufficiently large electric field causes electron-positron pair production. We discuss this analogy and describe the implications of this analysis for the mechanics of biopolymer filament bundles of various types under compression.

Long, stiff filaments held together by strong bonds are ubiquitous in biology. These filaments appear in both the cytoskeleton and the extracellular matrix in the form of bundles bound by a variety of cross-linking molecules, which, due to their weaker interactions with the filaments, attach and detach from the bundle reaching a chemical equilibrium with their concentration in the surrounding fluid. The mechanical response of filaments and their networks is well understood. The filaments are nearly inextensible; they respond to tensile or compressive loading by reducing or increasing (respectively) the amount of filament arc length stored in their transverse thermal undulations [1–4].

The collective mechanical response of filament bundles is more complex than that of simple elastic rods. For instance, bundles have a length-scale-dependent bending modulus [5], whereas the underlying filaments typically do not. The increased thickness of the bundle suppresses collective bending deformations, so bundles are significantly less compliant than their constituent filaments. But bundles admit new internal degrees of freedom associated with the filament reorganization. There are two relevant defects associated with these rearrangements: braids, corresponding to the transposition of filaments within the bundle, and loops, which trap extra length in a subset of the bundle's filaments between consecutive cross-links [6]. See Figs. 1(c) and 1(d) for schematic diagrams of pairs of loops and braids, respectively. Forming these defects from a quench by adding cross-linkers is commonplace, but since the addition or removal of these defects requires a system-sized rearrangement of cross-linkers, one cannot expect them to form spontaneously. Rather, they form in defect-antidefect pairs, which require only local cross-linker rearrangements. Since these defect pairs are associated with kinks, compressive loading suppresses the energy barrier associated with defect pair production. As a result, at a critical compressive stress, we expect defect pair proliferation once the energy cost of pair production is reduced to the thermal energy.

Stiff rods under compression are known to undergo a mechanical instability—Euler buckling [7,8]. We find that Euler buckling is precluded in bundles by another type of instability: at compressive stresses lower than the Euler buckling threshold, the bundles shorten by the thermally activated production of pairs of topological defects, leading to localized regions of bending deformation—*kinks*—unlike the system-sized bends encountered in Euler buckling.

Defect pair production is analogous to the Schwinger effect, in which electron-positron pair production was predicted in a sufficiently strong static electric field [9,10]. The forces due to the large electric field on the charged particle pairs pull them apart, stabilizing these quantum fluctuations of the vacuum. In the same way, it is energetically favorable for thermally generated defects to be produced under bundle compression. We term this mechanism the "thermal Schwinger effect."

To preserve the cross-linking structure far away from a defect pair, the length stored by defects must be conserved, so each defect carries a conserved scalar charge associated with length. A loop defect takes up excess length and its antidefect returns it. Similarly, braids carry a charge associated with the modified braid group. To preserve the cross-linking structure far away from the defect pair, the net braid charge of the defects must vanish; i.e., the braid-antibraid pair must be associated with inverse operations of the braid group. Each defect in a three-filament bundle then carries a charge from the product group $Br_3 \times Z_2 \times \mathbb{R}^2$ (see Supplemental Material [11]). In the following, loops refer to defects with zero braid-group charge, and braids carry the scalar length charge necessary to minimize their defect
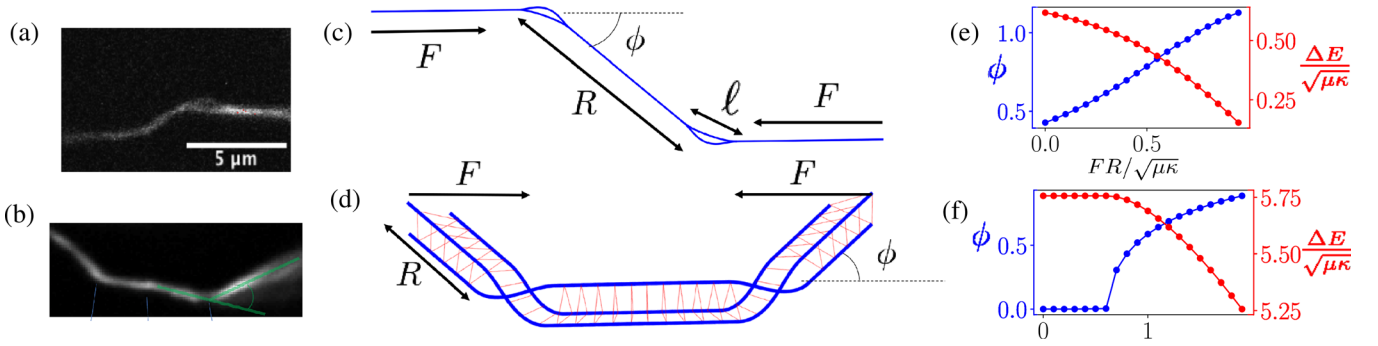
FIG. 1. Fluorescence microscopy images of a z bend (a) and a u bend (b) in a collagen bundle. (c) Two loops under compression form a z bend. (d) Two braids under compression form a u bend. (e) Angle ϕ produced by a loop pair (blue, left axis) and energy difference between the looped and straight bundle as a function of dimensionless torque (red, right axis). (f) Angle ϕ produced by a braid pair (blue, left axis) and the energy difference between braided and straight bundles as the function of dimensionless torque (red, right axis). (Images courtesy of E. Botvinick and Q. Hu.) (b) is reused from [6].

core energy. We leave more complex defect structures to future work. Defect pair production shortens the end-to-end distance of the bundle through the length stored in the defects' cores and in the bundle's kinking at the defects, reducing the formation energy cost of the defect pair under compression. Compression is the analog of the applied electric field in the Schwinger effect since it decreases the energy cost of defect pair production. For the case of current interest, the defect pairs are created by thermal, not quantum, fluctuations. Loop defects separate under compression, like the electron-positron pairs in the applied electric field. Braids, however, attract each other, forming bound states, which has no analog in the standard Schwinger effect.

We first consider production energy of loop and braid defects in a compressed bundle in order to compute the loop pair production rate at temperature T in a calculation reminiscent of the Kramers escape problem [12,13]. To compute the minimal energy configuration for stable and metastable states of the N-filament bundle under a compressive force F, we introduce the energy

$$E = -F\Delta L + \mu\ell + \sum_{i=1}^{N} \int ds \frac{\kappa_i}{2}(\partial_s \hat{t}_i)^2. \qquad (1)$$

The first term gives the energy reduction due to the shortening of the bundle's end-to-end distance ΔL. The cross-linkers have binding energy μ per unit length. Since defects disrupt cross-linking over a distance ℓ, their presence increases the system's energy as reflected by the second term on the right-hand side of Eq. (1). The third term gives the bending energy stored in the bundle, where κ_i and $\hat{t}_i(s)$ are the bending modulus and tangent vector of the ith filament. s is the arc length along the bundle. We neglect torsion, so all defect energies are actually lower bounds. There will be a continuous spectrum of excited states due to trapped torsion.

We examine first a pair of loop defects while assuming the compressive load to be sufficiently weak so the

characteristics of the loop, i.e., the dependence of its kink angle and energy on its size, can be taken from our previous calculations in the zero-compression limit [6]. We discuss the effect of the changing angle later and in the Supplemental Material [11]. The kink angles generated by neighboring loops are equal and opposite, since the amounts of their trapped length have to be equal and opposite (which also makes the loop sizes equal, see Supplemental Material [11]). A pair of loops produce a "z bend" where parts of the bundle not lying between the loop pair are parallel and offset in the normal direction to the undeformed bundle—Figs. 1(a) and 1(c). This result holds even for bundles having filaments of differing bending moduli, as long as the excess trapped length in the loop is much smaller than the total length of the defected region. For simplicity, we focus on the case of equal bending moduli. Then the total energy of configuration with two loops of size $\ell/2$ each, generating kink angles ϕ, and separated by a distance R is

$$E_{\text{tot}} = g_1 \mu\ell - FR(1 - \cos\phi). \qquad (2)$$

The first term in Eq. (2) is the energy of the pair of loops of length $\ell/2$, with coefficient $g_1 \approx 1.48$ (see Supplemental Material [11]). The second term is the decrease of energy due to the compression [see Fig. 1(c)]. As long as $F \ll \mu$, it is not important whether we define R to be the distance between centers of loops or their edges, since the difference will be small in comparison with the first term. However, we pick R to be the distance between closest edges, so it is equal to zero when loops are not yet separated.

Loop formation involves cross-linker removal and filament bending, leading to an energy increase of $g_1 \mu\ell$ as the loop size ℓ increases. At some loop size ℓ_0, the two growing loops separate due to random fluctuations. Once separated, the loops can no longer exchange trapped length, so their lengths are now fixed at $\ell_0/2$ each (see Supplemental Material [11]). As the distance interloop

distance R of the z bend grows, the energy of the compressed bundle decreases due to shortening along the direction of the compressive force. We can consider this process as an escape from the potential well using x as a single reaction coordinate describing the growth of the loop sizes while they overlap and then their separation afterward

$$U(x) = \begin{cases} g_1\mu x, x < \ell_0 \\ g_1\mu\ell_0 - F(1 - \cos\phi)(x - \ell_0), x > \ell_0, \end{cases} \quad (3)$$

x grows with the sizes of the loops $x = \ell$ before separation (upper equality), and then describes the distance between the separated loops $x = R$ (lower equality). The effective potential for the growing loops increases linearly with loop size up to the final loop size ℓ_0 and then decreases linearly due to the shortening of bundle. Taking into account the change of the angle due to increasing torque leads to faster decrease of the potential, which accelerates pair production. Here we present the calculation for the lower limit of the production rate, when the angle is assumed to be constant, and consider the effect a changing angle in the Supplemental Material [11].

Treating pair production as a Kramers escape problem [12] in the potential Eq. (3), we compute the escape rate r, the rate of loop pair production in thermal equilibrium at a fixed compressive stress. We compute this rate as the inverse of the mean time to escape using the standard Kramers approach for an overdamped system,

$$r^{-1} = \frac{1}{D}\int_0^{x_0} dy e^{\beta U(y)} \int_0^y dz e^{-\beta U(z)}, \quad (4)$$

where x_0 is defined such that $U(x_0) = 0$ and $\beta = 1/k_B T$. We introduce a loop diffusion constant $D \propto k_{\text{off}}\Delta x^2$ in terms of k_{off}, the rate of cross-linker unbinding and the distance between consecutive binding sites of those cross-linkers along the filament Δx.

Performing the integral in Eq. (4) in the limit of small F/μ and ϕ (see Supplemental Material [11]), we obtain

$$r^{-1} = \frac{4}{D\beta^2 F^2\phi^4}\left(\frac{\tau\phi^2}{2g_1}e^{\eta\phi} + \eta\phi - 1 + e^{-\eta\phi}\right), \quad (5)$$

where we introduce the dimensionless parameters $\tau = F/\mu$ and $\eta = g_1 g_2 \beta\sqrt{\kappa\mu}$, with $g_2 \approx 4.8$ relating defect size to the kink angle it produces: $\ell = g_2\sqrt{(\kappa/\mu)}\phi$ (see Supplemental Material [11]). The pair production rate r vanishes as ϕ goes to zero since the potential barrier width diverges as $1/\phi^2$. Conversely, very large angle kink production is also suppressed ($r \to 0$ as $\phi \to \infty$) due to the increasing energy of the loop. The rate of pair production has a maximum at a finite angle—see Fig. 2. We obtain a prediction for the most commonly produced kink angles in z bends as a function of material parameters of the bundle and the applied compressive load. In the limit of weak

compression, the maximum loop pair production rate r_{max} (z-bend formation rate) occurs at angle $\phi^\star$ (see Supplemental Material [11] for details),

$$\phi^\star = \eta^{-1}\log\left(\frac{6g_1\eta^2}{\tau}\right), \quad (6)$$

$$r_{\text{max}} = \frac{D}{3}\left[\frac{\tau\log(\frac{6g_1\eta^2}{\tau})}{2\beta\kappa}\right]^2. \quad (7)$$

The production rate of the z bends increases as the compressive force squared and is rather sharply peaked—Fig. 2—as a function of angle, suggesting that, for fixed material parameters, including bundle sizes, one expects to observe a narrow range of z-bending angles. The most probable z-bend angle scales roughly as $k_B T/\sqrt{\kappa\mu}$; the binding energy of the linkers determines the typical observed angles for bundles of a fixed number of filaments. Finally, as the bundle size grows, the effective κ increases, driving the z-bend angles to zero.

We now examine the production of braid-antibraid pairs in a three-filament system. Within the lowest energy configuration of the braid, two of the filaments follow the same trajectory, allowing us to reduce the problem to that of studying two filaments in 2D. We call the case of two filaments with equal bending moduli a pseudobraid, reserving the name braid for the more physical but analytically less tractable case of unequal bending moduli $\kappa_1 = 2\kappa_2$. See Ref. [6] for further details.

Unlike in the case of loops, only the magnitude of the kink angles produced by the braid pair must be equal. The kink angles generated by braids thus do not have to form z bends; in fact, the lowest energy state will be a u bend, as shown in Fig. 1(b). This energy is minimized when the two defects are close to each other and localized in the middle of the bundle, since this provides the greatest shortening in response to the force. We speculate that braid defect colocalization is the primary reason for the rarity of u-bend observations as compared to z bends (see Ref. [6]). It could be easy to misinterpret u bends as a single defect with a larger kink angle.

To study braids, we introduce two dimensionless parameters: a material parameter $\zeta = (\mu a^2/\kappa)$ and an applied
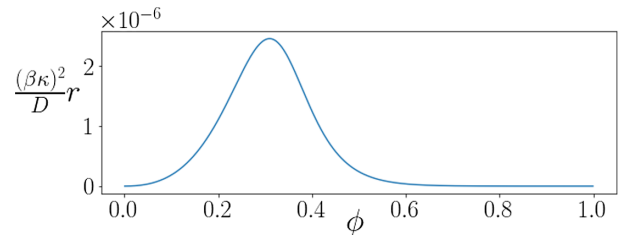
FIG. 2. Dimensionless loop pair production rate with $\eta \approx 22.5$, $\tau = 0.1$ [see Eq. (5)].

force $f = (FRa/\kappa)$, where a is the spacing between the centerlines of the filaments enforced by the cross-linkers. We find that, up to a critical compression $f^\star(\zeta)$, implicitly determined by

$$\int_0^1 \frac{\frac{(\zeta - \sqrt{2\zeta})^2}{f^2} t \, dt}{\sqrt{1 - \frac{(\zeta - \sqrt{2\zeta})^2}{f^2} t^2} \sqrt{1 - t}} = \sqrt{\zeta/2}, \qquad (8)$$

the minimum energy configuration of the braid-antibraid pair remains that of an unkinked bundle as shown in Fig. 1(f). This is distinct from the case of loop pairs where low-angle loops can form at any compressive load. For $f > f^\star(\zeta)$, the defect pairs produce finite-angle kinks making a u bend—Fig. 1(f).

Solving Eq. (8) numerically [which agrees with the numerical minimization of the energy Eq. (1)], we obtain a phase diagram spanned by compressive loading f and ζ shown in Fig. 3. The graph is the critical loading for u-bend formation versus linker binding energy μ at fixed κ and a. The nonmonotonic behavior of the curve can be understood as follows. For sufficiently large μ, kinks appear at braids even at zero compressive stress, but as the linker binding energy decreases, kink formation is energetically unfavorable unless the shortening of the bundle under load produces a sufficient energy reduction. For small enough linker binding energy, the defected regions extend in arc length, thereby becoming more bending compliant so that there is a reentrant kinking regime at small μ. The behavior of the more physical, asymmetric case (green circles) is similar to that of the pseudobraid (red circles and blue line), but the transition is shifted to higher compressive loads due to the increased bending rigidity of the system.

Upon increasing the compressive load, we predict that bundles should first shorten by producing loop pair defects creating z bends, as found in the collagen bundles seen in Fig. 1(a). Assuming the size of the bundles is known and controlled, the resulting z bends will be generated with reproducible angles, due to the peak in stochastic defect
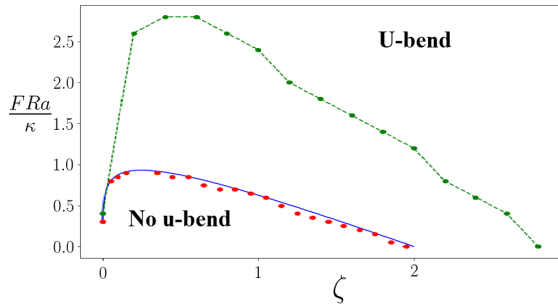
FIG. 3. Numerical minimization of the energy (red dots) and analytical prediction [Eq. (8)] for a symmetric pseudobraid $\kappa_1 = \kappa_2$. The numerical solution of the more complex, three-filament braid with $\kappa_1 = 2\kappa_2$ (green circles) shows that the transition is shifted to higher compression.

production rate with angle as shown in Fig. 2. The high polydispersity of typical biopolymer filament bundles should spread out the distribution of z-bend angles. But since the angle of maximum production $\phi^\star \sim k_B T / \sqrt{\kappa \mu}$ and for a bundle of N filaments $\kappa \sim N^2$, we expect $\delta \phi^\star \sim \delta N N^{-2}$. The peak in the z-bend angle distribution may be hard to observe without some bundle control unless N is large. If the cross-linking energy is sufficiently large, the z-bend angles will vanish as $\phi \sim 1/\mu^{1/2}$. However, as the distance R between the two loops increases, we cannot continue to neglect the increase of the equilibrium loop angle shown in Fig. 1(e), which may lead to observable angles at large R, even if they were unobservably small angles at formation. As shown in the Supplemental Material [11], loop pairs will generically deform to sharp angles—crumple—as they separate. Such large angles have not been observed in collagen bundles [6]. This may be due to one of two possibilities. The bundles may be short enough that z bends would have to diffuse off the ends to reach sufficient torque for crumpling, or defect motion may be so slow that their equilibrium state is not typically observed.

At higher compression, the u bends seen in Fig. 1(b) will also be created when braid pair production is reduced to thermal energy. One may ask whether braids or loops are preferentially generated under particular conditions of fixed torque. Defect formation is an inherently stochastic process, but we expect that, since there is a continuous spectrum of low-energy, small stored length loops, these should form preferentially at lower temperatures. To further examine this point, we provide in the Supplemental Material [11] a phase diagram showing that loops storing small amounts of excess length, leading to smaller kink angles ϕ, are energetically favored over braid pair production when the loop kink angles remain below a threshold $\phi(\zeta)$.

Using estimates of $\zeta \sim 0.1$ [6] for filamentous actin (F-actin) and collagen, we predict uncompressed bundles support unkinked braids. Braid pair production leading to u-bend formation should occur for compressive forces on the order of 10 pN based on the phase diagram shown in Fig. 3. DNA condensed by polyvalent ions and cross-linked intermediate filaments have $\zeta \sim 100$ [6], suggesting that there will be a number of kinked braids quenched into the bundle. As a result, we expect these bundles to collapse by bending at the preexisting braids, which introduce more bending compliant regions via cross-linker reduction. Finally, we note that under sufficiently large forces, Euler buckling can take over from braid-generated u-bend formation. We estimate that Euler buckling should be found for $FRa/\kappa \approx 5$ (see Supplemental Material [11]) for $\zeta \approx 0.1$ (this value increases with ζ), which is well above the region shown in the u-bend phase diagram, Fig. 3.

The most direct test of the theory should be found in compression experiments on individual bundles. For collagen and F-actin, the necessary compressive forces are on

the order of 10 pN, suggesting laser trapping experiments as a probe. There remain a number of open questions about more complex defects and their interactions on the bundle. More complex defects containing excess length and braids may form and may exchange length via the transport of pure loop defects between them. Finally, since cytoskeletal bundles are often found in conjunction with molecular motors, one may ask how motor-induced forces drive defect dynamics.

---

[1] F. C. MacKintosh, J. Käs, and P. A. Janmey, Elasticity of Semiflexible Biopolymer Networks, Phys. Rev. Lett. **75,** 4425 (1995).

[2] D. C. Morse, Viscoelasticity of tightly entangled solutions of semiflexible polymers, Phys. Rev. E **58,** R1237 (1998).

[3] R. Everaers, F. Jülicher, A. Ajdari, and A. C. Maggs, Dynamic Fluctuations of Semiflexible Filaments, Phys. Rev. Lett. **82,** 3717 (1999).

[4] C. P. Broedersz and F. C. MacKintosh, Modeling semiflexible polymer networks, Rev. Mod. Phys. **86,** 995 (2014).

[5] C. Heussinger, M. Bathe, and E. Frey, Statistical Mechanics of Semiflexible Bundles of Wormlike Polymer Chains, Phys. Rev. Lett. **99,** 048101 (2007).

[6] V. M. Slepukhin, M. J. Grill, Q. Hu, E. L. Botvinick, W. A. Wall, and A. J. Levine, Topological defects produce kinks in biopolymer filament bundles, Proc. Natl. Acad. Sci. U.S.A. **118,** e2024362118 (2021).

[7] L. D. Landau and E. M. Lifshitz, *Course of Theoretical Physics*, Theory of Elasticity, 3rd ed. (Butterworth-Heinemann, Oxford, 1986), Vol. 7.

[8] L. Golubović, D. Moldovan, and A. Peredera, Dynamics of the Euler Buckling Instability, Phys. Rev. Lett. **81,** 3387 (1998).

[9] J. Schwinger, On gauge invariance and vacuum polarization, Phys. Rev. **82,** 664 (1951).

[10] J. Schwinger, The theory of quantized fields. V, Phys. Rev. **93,** 615 (1954).

[11] See Supplemental Material at http://link.aps.org/supplemental/10.1103/PhysRevLett.127.157801 for calculation details.

[12] H. A. Kramers, Brownian motion in a field of force and the diffusion model of chemical reactions, Physica (Utrecht) **7,** 284 (1940).

[13] N. V. Kampen, *Stochastic Processes in Physics and Chemistry* (North Holland, Amsterdam, 2007).